A V-Shaped Small Molecule-Based Crystalline Nonporous Supramolecular Organic Framework for Capturing Benzene-Based Contaminants

Jin-Fa Chen,* Yuxuan Wang, Bingbing Shi, Hong Yao, Tai-Bao Wei and Qi Lin*

Key Laboratory of Eco-Environment-Related Polymer Materials, Ministry of Education of China; Key Laboratory of Polymer Materials of Gansu Province; College of Chemistry and Chemical Engineering, Northwest Normal University, Lanzhou, Gansu 730070, P. R. China. E-mail: chenjinfa@nwnu.edu.cn, linqi2004@126.com.

Table of Contents

1. Materials and methods

All reagents were commercially available and used as supplied without further purification. Solvents were either employed as purchased or dried according to procedures described in the literature.

^{1}H NMR and ^{13}C HMR spectra were recorded with a Bruker Avance DMX-600 spectrometer, a Bruker Avance DMX-400 using the deuterated solvent as the lock and the residual solvent or TMS as the internal reference.

High-resolution mass spectrometric experiments were performed with a Bruker 7-Tesla FT-ICR mass spectrometer equipped with an electrospray source (Billerica, MA, USA).

Thermogravimetric Analysis (TGA) analysis was carried out using a Q5000IR analyzer (TA instruments) with an automated vertical overhead thermobalance. The samples were heated at the rate of 10 °C/min using N_2 as the protective gas.

N_2 isotherm was generated by incremental exposure to ultra high purity nitrogen up to 1.0 atm in a liquid nitrogen bath (77.3 K), and surface parameters were determined using BET adsorption models included in the instrument software (BELSORP-Max).

Powder X-ray diffraction (PXRD) data were collected in transmission mode on samples held on thin Mylar film in aluminum well plates on a Panalytical X'Pert PRO MPD equipped with a high throughput screening (HTS) XYZ stage, X-ray focusing mirror, and PIXcel detector, using Ni-filtered Cu Kα radiation.

Gas chromatographic analysis was performed using an Agilent 7890A-5975C instrument equipped with an HP-INNOWAX column (60.0 m × 250 μm, 0.25 μm). The method of gas chromatography used was as follows: the starting temperature was held at 40°C for 3 min, increased to 100°C at a rate of 5°C/min, increased to 230°C at a rate of 10°C/min and held for 5 min, the gasification chamber temperature was 250°C, the temperature of the transfer line was 240°C, and the carrier gas, He, was used with a carrier gas flow rate of 1 mL/min, without splitting the flow.

Single crystal growth was performed via the following methods:

(a) **1**: Weigh 6 mg of pure compound **1** in a 10 mL glass vial, add 2.5 mL of analytically pure methylene chloride and heat to dissolve until the solution is clear and transparent, then add 2.5 mL of analytically pure *n*-hexane to the glass vial, unscrew the cap, and cultivate single crystals by allowing the solvent to evaporate slowly.

(b) **Bz@1**: 5.0 mg of **1** dry powder is placed in a vial and 5 ml of benzene solution is added. **Bz@1** crystals are obtained by slow evaporation of the solution.

(c) **ToL@1**: 5.0 mg of **1** dry powder is placed in a vial and 5 ml of toluene solution is added. **ToL@1** crystals are obtained by slow evaporation of the solution.

(d) **oXL@1**: 5.0 mg of **1** dry powder is placed in a vial and 5 ml of o-xylene solution is added. **oXL@1** crystals are obtained by slow evaporation of the solution.

(e) **mXL@1**: 5.0 mg of **1** dry powder is placed in a vial and 5 ml of m-xylene solution is added. **mXL@1** crystals are obtained by slow evaporation of the solution.

(f) **pXL@1**: 5.0 mg of **1** dry powder is placed in a vial and 5 ml of p-xylene solution is added. **pXL@1** crystals are obtained by slow evaporation of the solution.

2. Synthesis of 1

The mixture of 2,9-dibromo-1,10-phenanthroline (338 mg, 1.0 mmol), 4-(9-carbazolyl)phenylboric acid (718 mg, 2.5 mmol), $Pd(PPh_3)_4$ (231 mg, 0.2 mmol), and K_3PO_4 (318 mg, 1.5 mmol) in 1,4-dioxane/H_2O (15 mL/3 mL) was refluxed in an oil bath with stirring under N_2 for 24 h. The reaction mixture was then cooled to room temperature and poured into water (30 mL). After extraction with CH_2Cl_2, the combined organic phases were dried over Na_2SO_4. Purification by column chromatography on silica gel (petroleum ether/ethyl acetate = 40:1, v/v) gave **1** as a light yellow solid (1,464 mg, 70%). M.p. 213–215 ºC. ^{1}H NMR spectrum of **1** is shown in Figure S1. ^{1}H NMR (400 MHz, Chloroform-*d*) δ 8.70 (d, *J* = 8.5 Hz, 4H), 8.42 (d, *J* = 8.4 Hz, 2H), 8.26 (d, *J* = 8.4 Hz, 2H), 8.16 (d, *J* = 7.7 Hz, 4H), 7.88 (s, 2H), 7.82 (d, *J* = 8.5 Hz, 4H), 7.55 (d, *J* = 8.2 Hz, 4H), 7.48–7.42 (m, 4H), 7.33–7.28 (m, 4H). ^{13}C NMR spectrum of **1** is shown in Figure S2. ^{13}C NMR (151 MHz, Chloroform-*d*) δ 156.43, 149.09, 147.52, 136.78, 129.32, 128.59, 127.56, 125.63, 124.82, 123.34, 123.22. ESI-HRMS (m/z): calcd for $C_{48}H_{30}N_4$ 663.2543 ($M+H^+$), found 663.2527 ($M+H^+$).

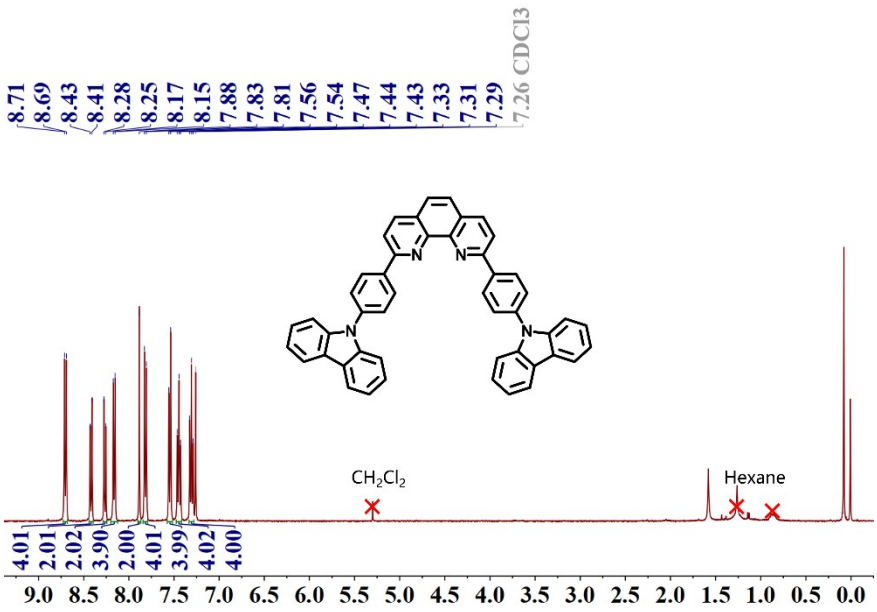

Figure S1. ^{1}H NMR spectrum (400 MHz, $CDCl_3$, 298 K) of compound **1**.

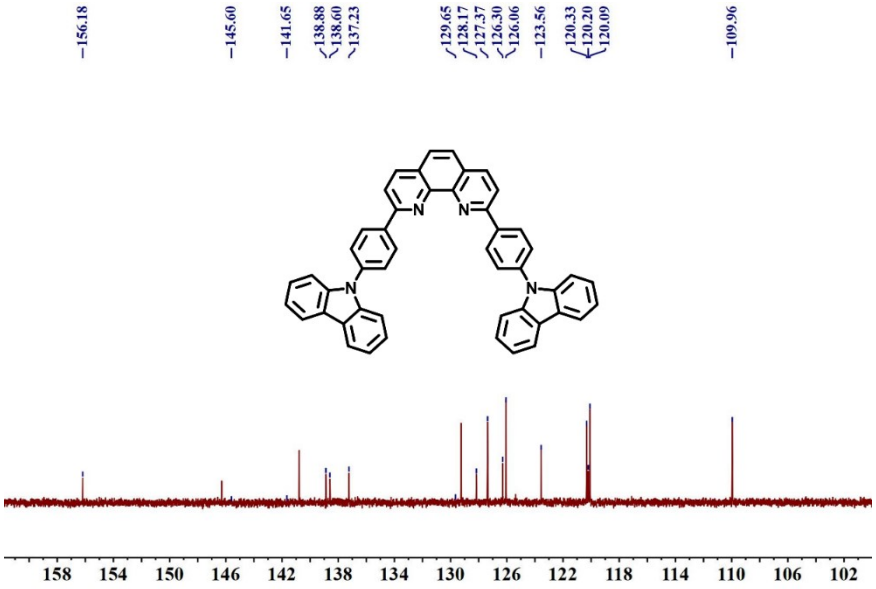

Figure S2. ^{13}C NMR spectrum (151 MHz, $CDCl_3$, 298 K) of compound **1**.

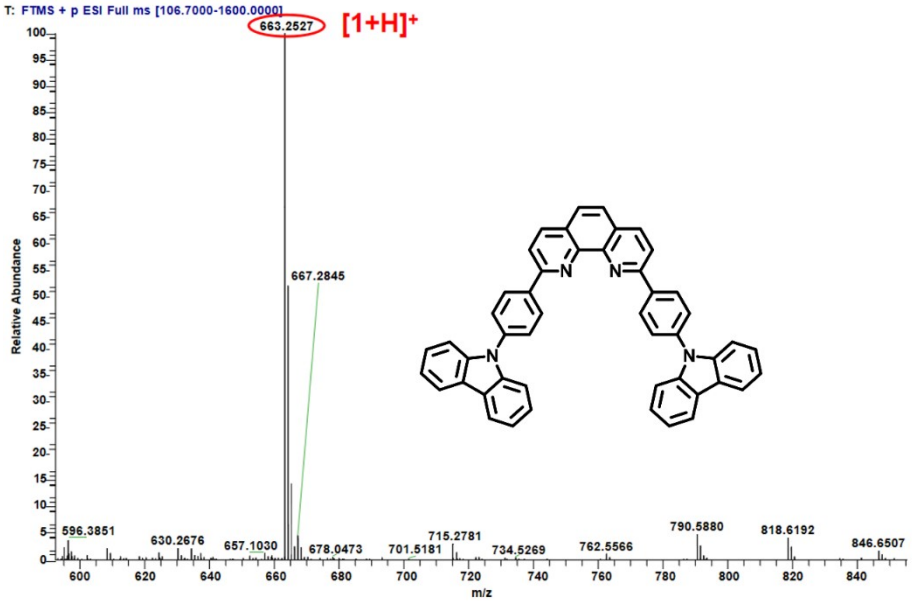

Figure S3. HRMS spectrum for **1**. Assignment of the main peak: *m/z* 663.2527 [**1**+H]$^+$.

3. Self-assembled single-crystal structure of 1

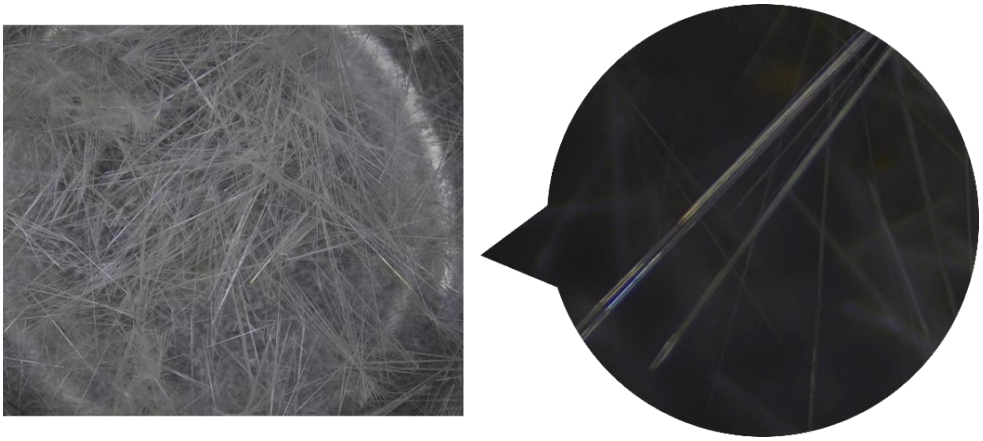

Figure S4. Pictures of single crystals of high-quality transparent compound **1** obtained by slow evaporation in a mixture of CH_2Cl_2/hexane (1:1, v/v).

Crystal Structure Determination:

Single-crystal X-ray diffraction data was collected on an XtaLAB Synergy R diffractometer. The CrysAlisPro software suite was used to manage data collection, reduction (SAINT V8.38A1), absorption correction by the Multi-scan method (SADABS), structure determination *via* direct methods (SHLEXT) and model refinement (SHELXL). All nonhydrogen atoms were refined anisotropically and all hydrogen atoms were refined with isotropically with their positions constrained to their carriers. Platon Squeeze was used to account for regions of heavily disordered solvent that could not be modlled. Supplementary CIFs, which include structure factors, are available free of charge from the Cambridge Crystallographic Data Centre (CCDC) *via* www.ccdc.cam.ac.uk/data_request/cif.

Table S1. *X-ray* Crystallographic data.

	1	**Bz@1**	**ToL@1**	**oXL@1**	**mXL@1**	**pXL@1**
CCDC	2429112	2429113	2429114	2429115	2429116	2429117
Empirical formula	$C_{50}H_{34}Cl_4N_4$	$C_{66}H_{48}N_4$	$C_{55}H_{38}N_4$	$C_{56}H_{40}N_4$	$C_{56}H_{40}N_4$	$C_{56}H_{40}N_4$
Formula weight	832.61	897.08	754.89	768.92	768.92	768.92
Temperature/K	150.00(10)	150.00(10)	150.00(10)	150.00(10)	150.00(10)	150.00(10)
Crystal system	orthorhombic	monoclinic	orthorhombic	orthorhombic	monoclinic	orthorhombic
Space group	$Cmc2_1$	$P2_1/c$	$Cmc2_1$	$Pna2_1$	$P2_1$	$Cmc2_1$
a/Å	29.9340(8)	29.0124(7)	30.1235(7)	15.9030(2)	15.4109(4)	29.6967(6)
b/Å	15.0767(5)	9.1087(2)	14.8515(4)	28.7810(4)	8.6328(2)	15.1954(3)
c/Å	8.7946(2)	19.0026(4)	8.8086(2)	8.88980(10)	16.4219(5)	8.9495(2)
α/°	90	90	90	90	90	90
β/°	90	107.111(2)	90	90	111.528(3)	90
γ/°	90	90	90	90	90	90
Volume/Å^3	3969.05(19)	4799.45(19)	3940.78(17)	4068.90(9)	2032.34(10)	4038.49(15)
Z	4	4	4	4	2	4
ρ_{calc}g/cm^3	1.393	1.242	1.272	1.255	1.256	1.265
μ/mm^{-1}	3.040	0.555	0.575	0.566	0.566	0.570
F(000)	1720.0	1888.0	1584.0	1616.0	808.0	1616.0
Crystal size/mm^3	0.12 × 0.05 × 0.04	0.15 × 0.06 × 0.05	0.19 × 0.15 × 0.12	0.12 × 0.08 × 0.05	0.12 × 0.05 × 0.03	0.18 × 0.08 × 0.05
Radiation	Cu Kα (λ = 1.54184)	Cu Kα (λ = 1.54184)	Cu Kα (λ = 1.54184)	Cu Kα (λ = 1.54184)	Cu Kα (λ = 1.54184)	Cu Kα (λ = 1.54184)
2Θ range for data collection/°	5.904 to 153.116	3.186 to 157.432	11.918 to 152.624	6.142 to 152.666	5.786 to 152.508	6.534 to 152.656
Index ranges	-36 ≤ h ≤ 27 -19 ≤ k ≤ 19 -10 ≤ l ≤ 4	-36 ≤ h ≤ 36 -10 ≤ k ≤ 11 -20 ≤ l ≤ 23	-37 ≤ h ≤ 36 -18 ≤ k ≤ 18 -6 ≤ l ≤ 10	-18 ≤ h ≤ 19 -32 ≤ k ≤ 35 -10 ≤ l ≤ 10	-19 ≤ h ≤ 19 -7 ≤ k ≤ 10 -20 ≤ l ≤ 20	-35 ≤ h ≤ 37 -18 ≤ k ≤ 18 -7 ≤ l ≤ 10
Reflections collected	6494	9510	13292	26555	28343	7121
Independent reflections	2850 [R_{int} = 0.0809, R_{sigma} = 0.0663]	9510 [R_{int} = 0.0619, R_{sigma} = 0.0482]	2981 [R_{int} = 0.0628, R_{sigma} = 0.0407]	7318 [R_{int} = 0.0331, R_{sigma} = 0.0285]	6788 [R_{int} = 0.0386, R_{sigma} = 0.0305]	2963 [R_{int} = 0.0315, R_{sigma} = 0.0340]
Data/restraints/parameters	2850/1/2235	9510/0/633	2981/35/272	7318/1/543	6788/517/619	2963/55/310
Goodness-of-fit on F^2	1.099	1.112	1.069	1.037	1.038	1.064
Final R indexes [I>=2σ (I)]	R_1 = 0.0829, wR_2 = 0.2293	R_1 = 0.0962, wR_2 = 0.2730	R_1 = 0.0601, wR_2 = 0.1536	R_1 = 0.0342, wR_2 = 0.0870	R_1 = 0.0344, wR_2 = 0.0887	R_1 = 0.0342, wR_2 = 0.0854
Final R indexes [all data]	R_1 = 0.0894, wR_2 = 0.2368	R_1 = 0.1168, wR_2 = 0.2824	R_1 = 0.0738, wR_2 = 0.1685	R_1 = 0.0371, wR_2 = 0.0894	R_1 = 0.0392, wR_2 = 0.0920	R_1 = 0.0383, wR_2 = 0.0885
Largest diff. peak/hole/e Å^{-3}	0.54/-0.45	0.46/-0.39	0.47/-0.31	0.21/-0.18	0.15/-0.11	0.13/-0.12

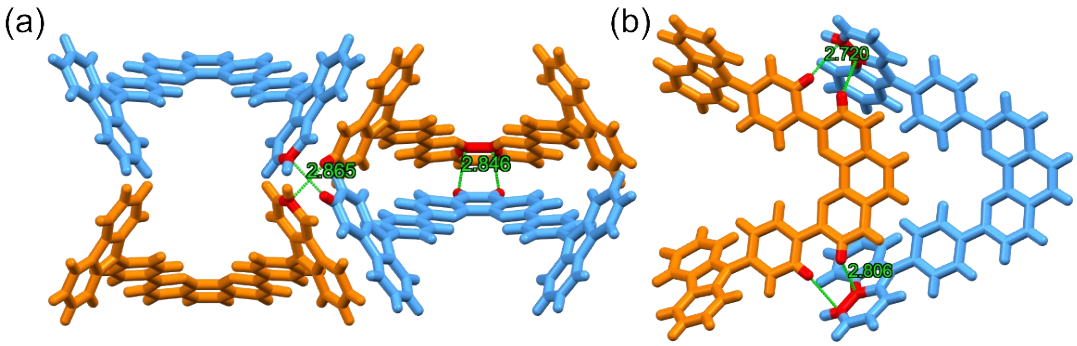

Figure S5. C-H···π interactions between neighboring **1** in the solid state.

4. PXRD and BET patterns of 1-SOFα crystals

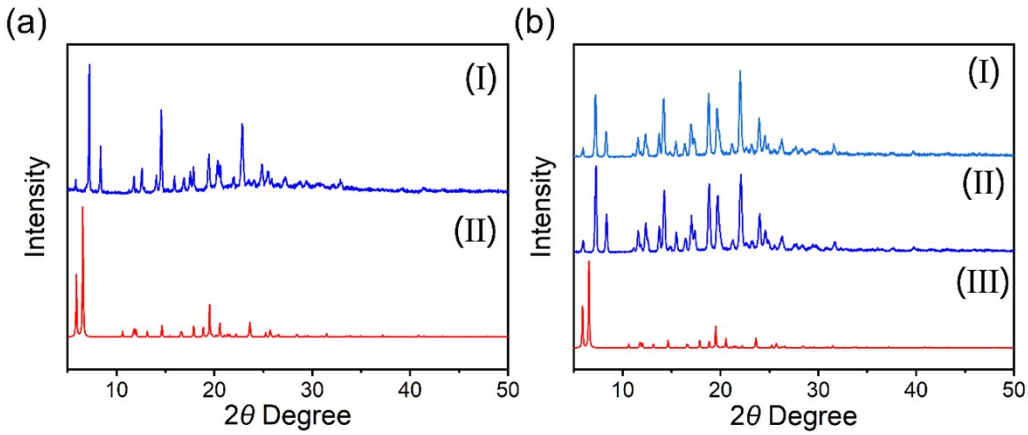

Figure S6. (a) PXRD patterns of **1-SOFα** crystals: (I) **1-SOFα** crystals were prepared by recrystallizing **1** and drying at 353 K for 4 hours; (II) simulated from single-crystal structure of **1**. (b) PXRD patterns of **1-SOFα**: (I) adsorption of water vapor after 48 hours; (II) **1-SOFα** crystals were prepared by recrystallizing **1** and drying at 353 K for 4 hours; (III) simulated from single-crystal structure.

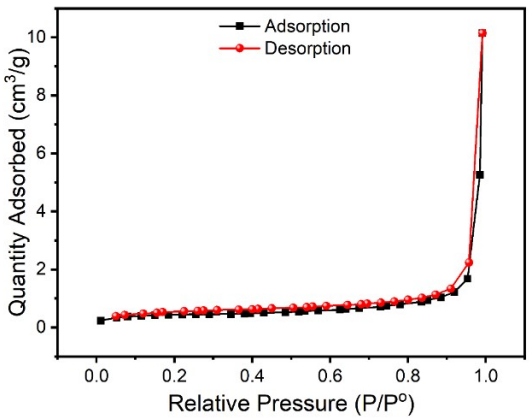

Figure S7. N_2 adsorption/desorption isotherms at 77 K measuring the porosity of **1-SOFα** crystals. (The specific surface area calculated by Brunner-Emmett-Taylor (BET) analysis was 1.62 $m^2\ g^{-1}$, and the adsorption cumulative volume of pores calculated by Barrett-Joyner-Hallenda (BJH) model was 0.0155 $cm^3\ g^{-1}$)

5. Thermogravimetric (TGA) measurements results

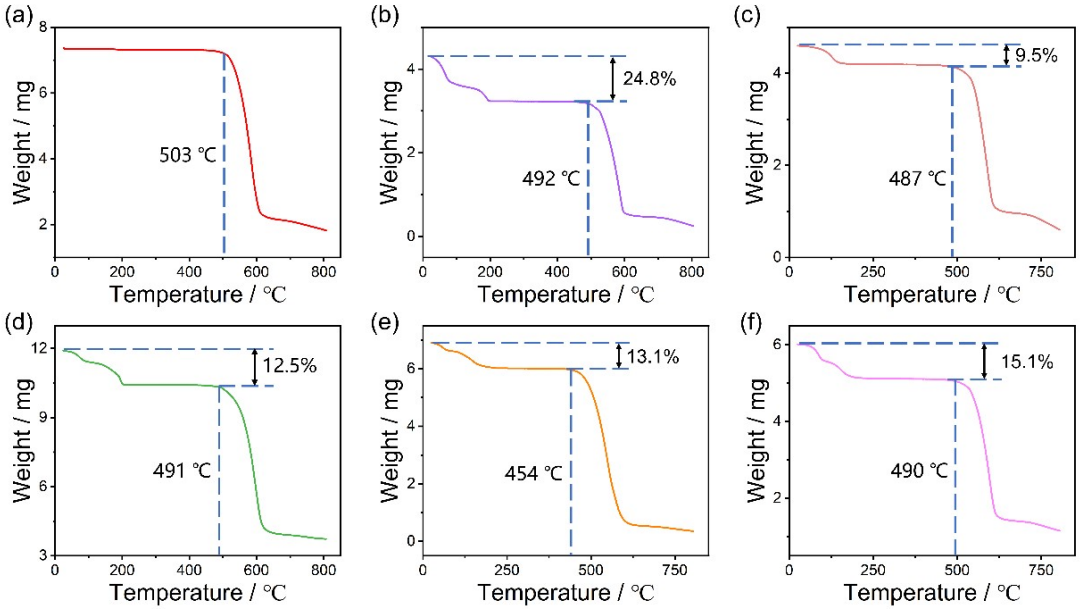

Figure S8. Thermogravimetric analysis of (a) **1-SOFα** crystals. (b) **Bz@1-SOFα**. (c) **ToL@1-SOFα**. (d) **oXL@1-SOFα**. (e) **mXL@1-SOFα**. (f) **pXL@1-SOFα**. There was no apparent weight loss happened for **1α** crystals below 503 °C. However, the weight losses of the BTX-adsorbed **1-SOFα** crystals below 503 °C were significant.

6. Single-crystal structures of BTX-loaded 1

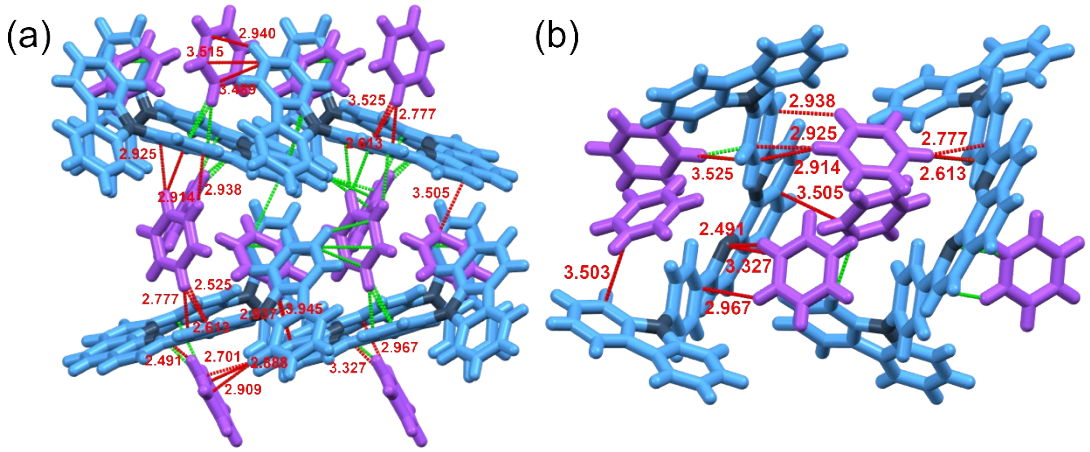

Figure S9. Single-crystal structures of **Bz@1**. (a) the *a*-axis view. (b) the *b*-axis view. The driving force is the C-H···π interaction.

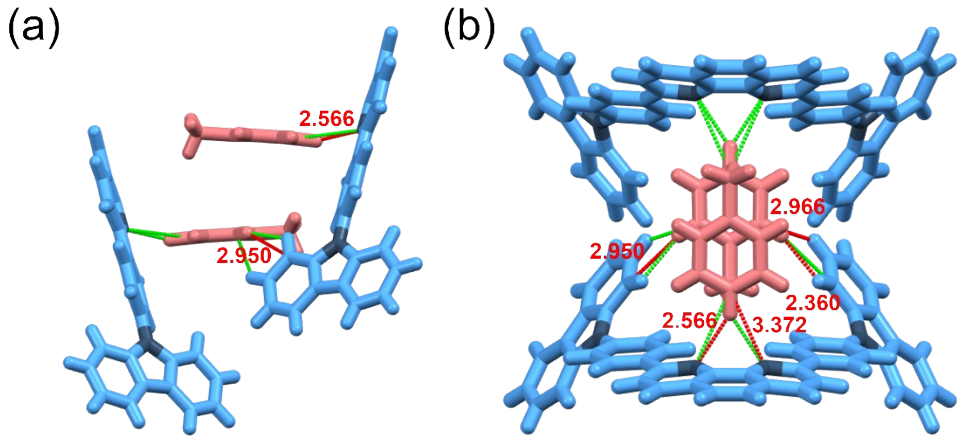

Figure S10. Single-crystal structures of **ToL@1**. (a) the *a*-axis view. (b) the *c*-axis view. The driving force is the C-H···π interaction.

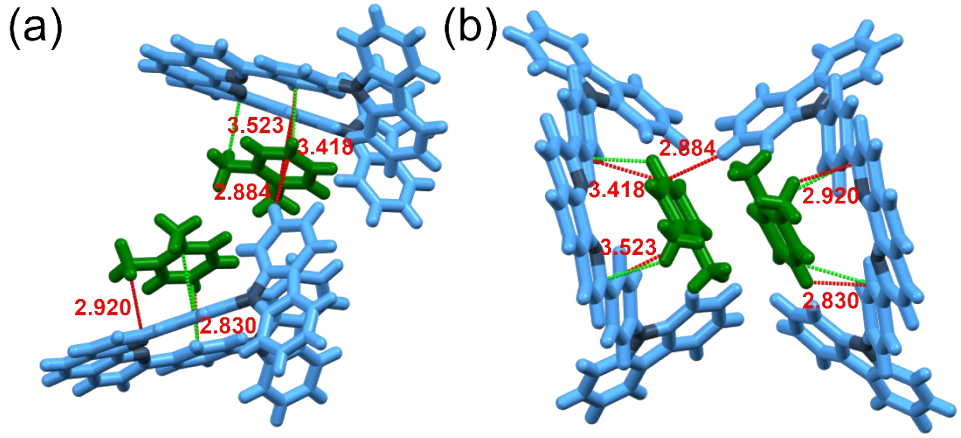

Figure S11. Single-crystal structures of **oXL@1**. (a) the *b*-axis view. (b) the *c*-axis view. The driving force is the C-H···π interaction.

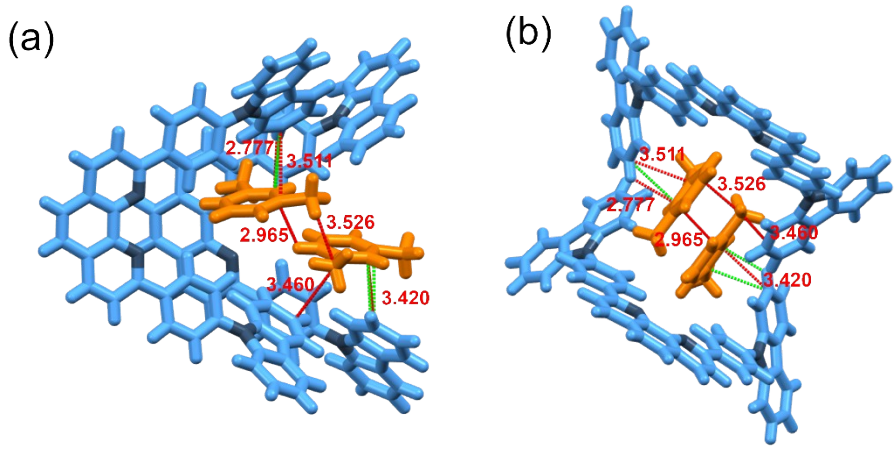

Figure S12. Single-crystal structures of **mXL@1**. (a) the *a*-axis view. (b) the *b*-axis view. The driving force is the C-H···π interaction.

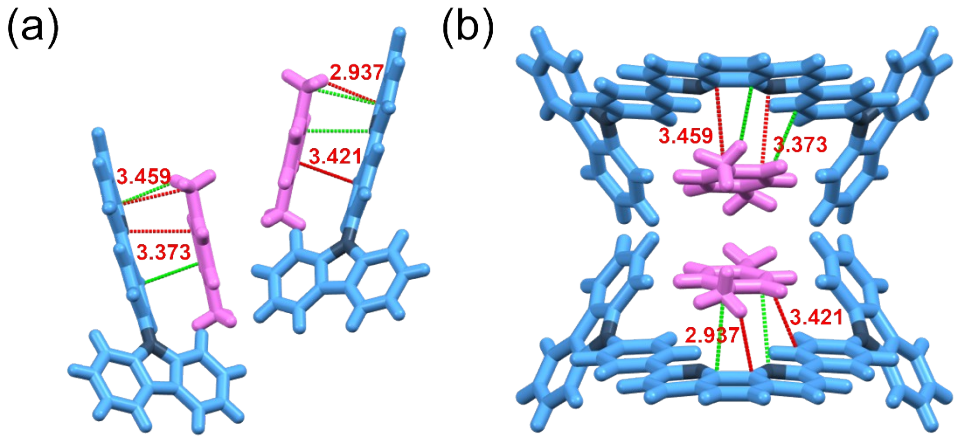

Figure S13. Single-crystal structures of **pXL@1**. (a) the *a*-axis view. (b) the *c*-axis view. The driving force is the C-H···π interaction.

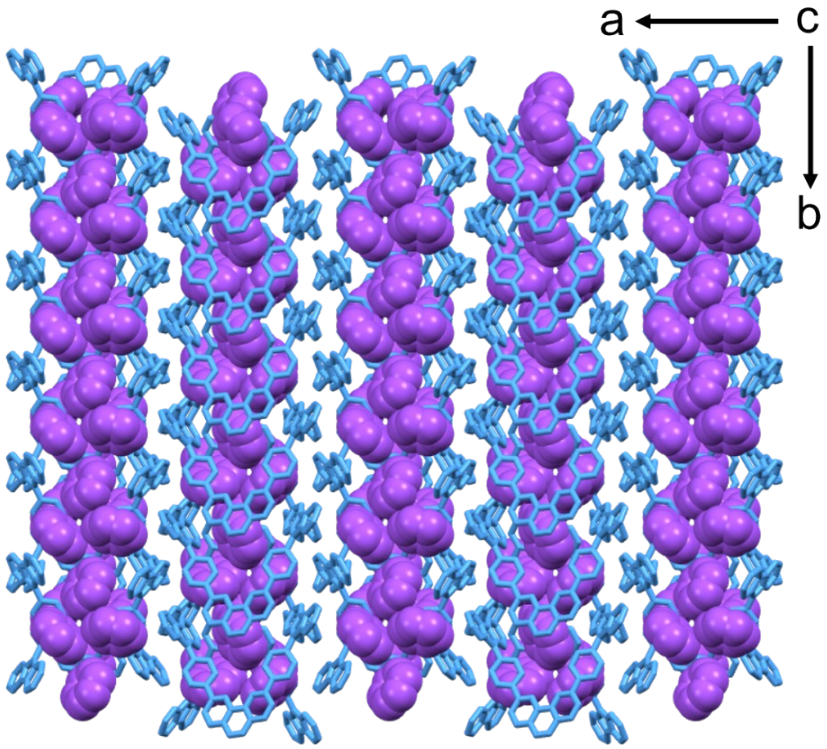

Figure S14. Single-crystal packing structure of **Bz@1** along *c*-axis. Hydrogen atoms are omitted for clarity.

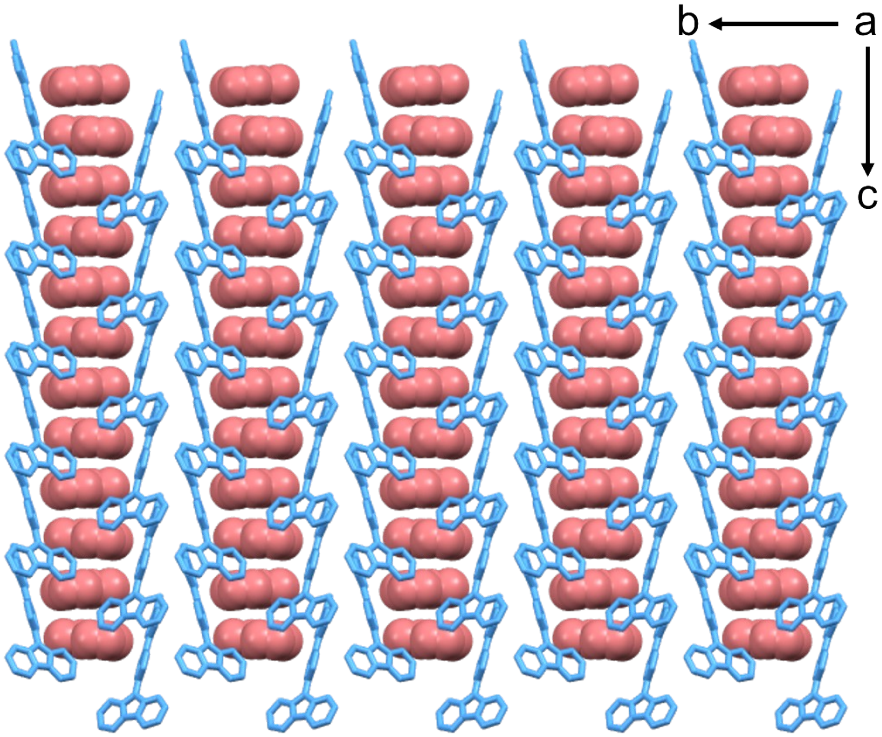

Figure S15. Single-crystal packing structure of **ToL@1** along *a*-axis. Hydrogen atoms are omitted for clarity.

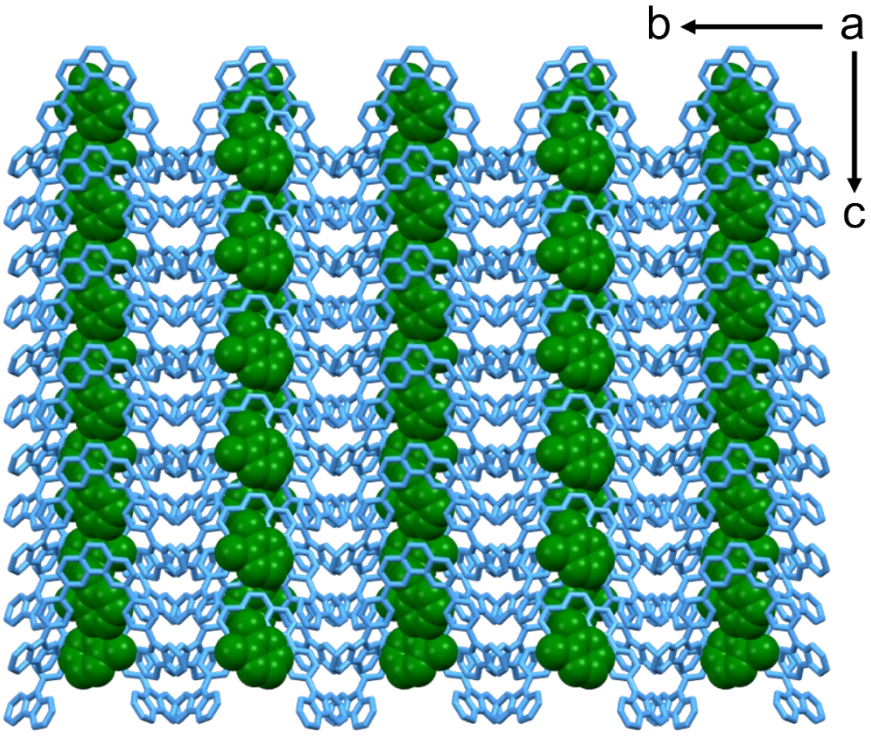

Figure S16. Single-crystal packing structure of **oXL@1** along *a*-axis. Hydrogen atoms are omitted for clarity.

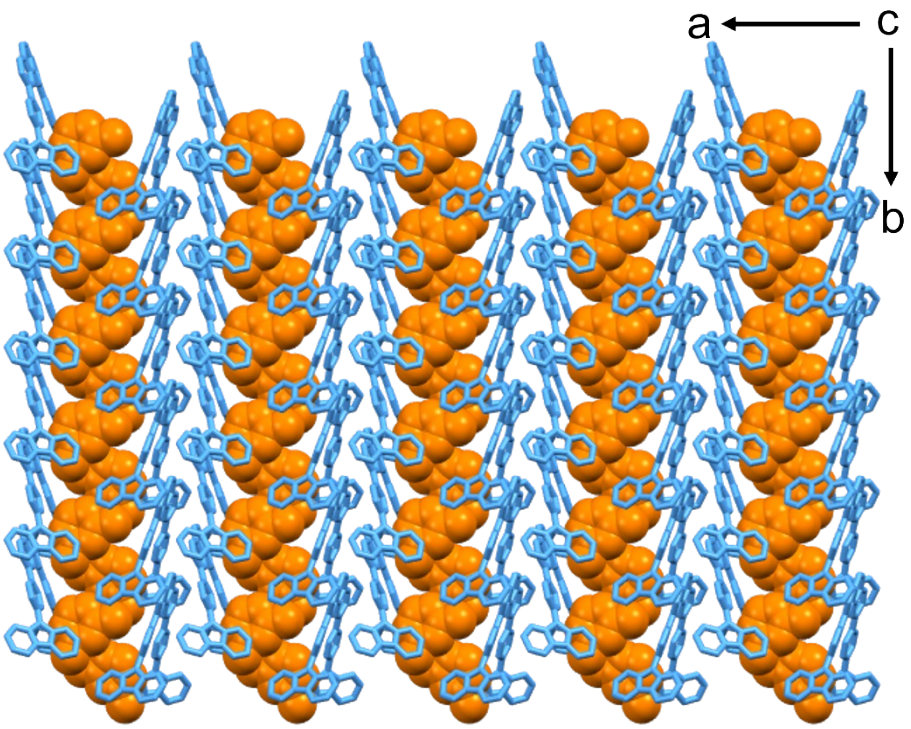

Figure S17. Single-crystal packing structure of **mXL@1** along *c*-axis. Hydrogen atoms are omitted for clarity.

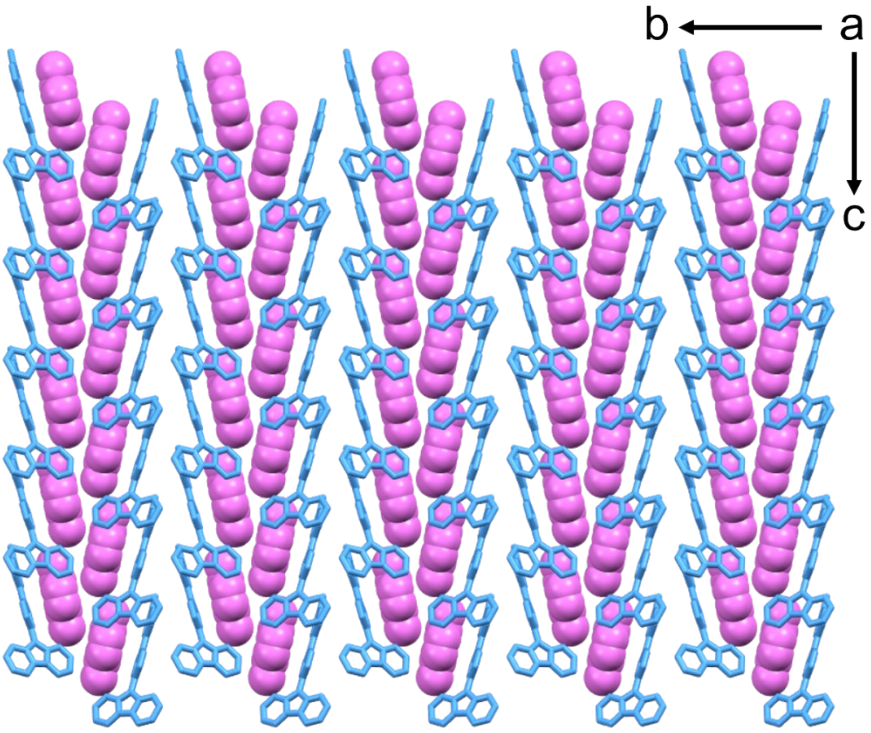

Figure S18. Single-crystal packing structure of **pXL@1** along *a*-axis. Hydrogen atoms are omitted for clarity.

7. Host–guest studies between 1 and BTX in solution

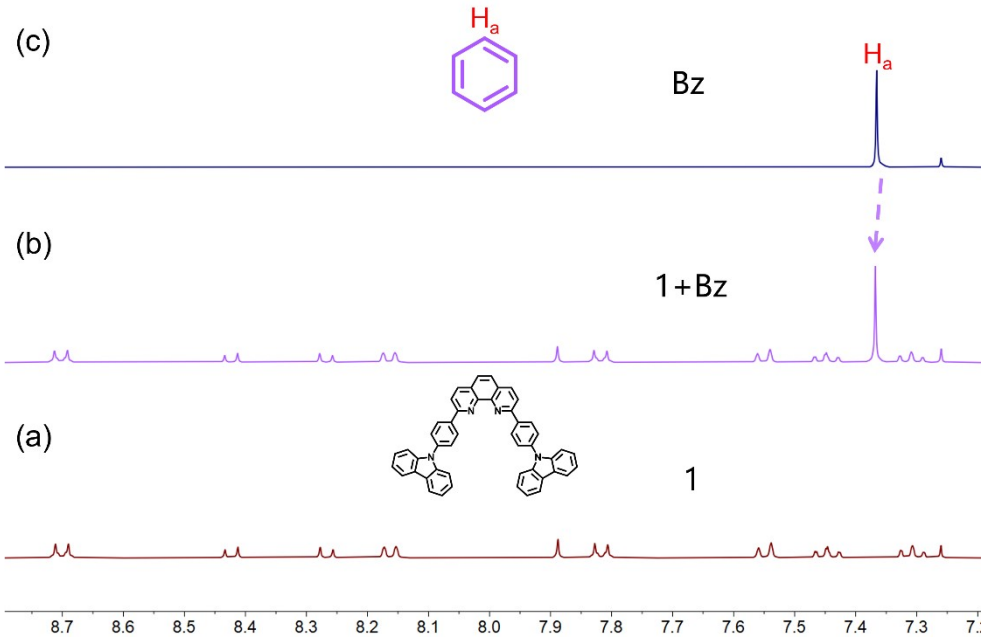

Figure S19. Partial ^{1}H NMR (400 Hz, $CDCl_3$, 298 K) spectra: (a) **1** (9.06 mM); (b) **1** (9.06 mM) and Bz (18.12 mM); (c) Bz (18.12 mM).

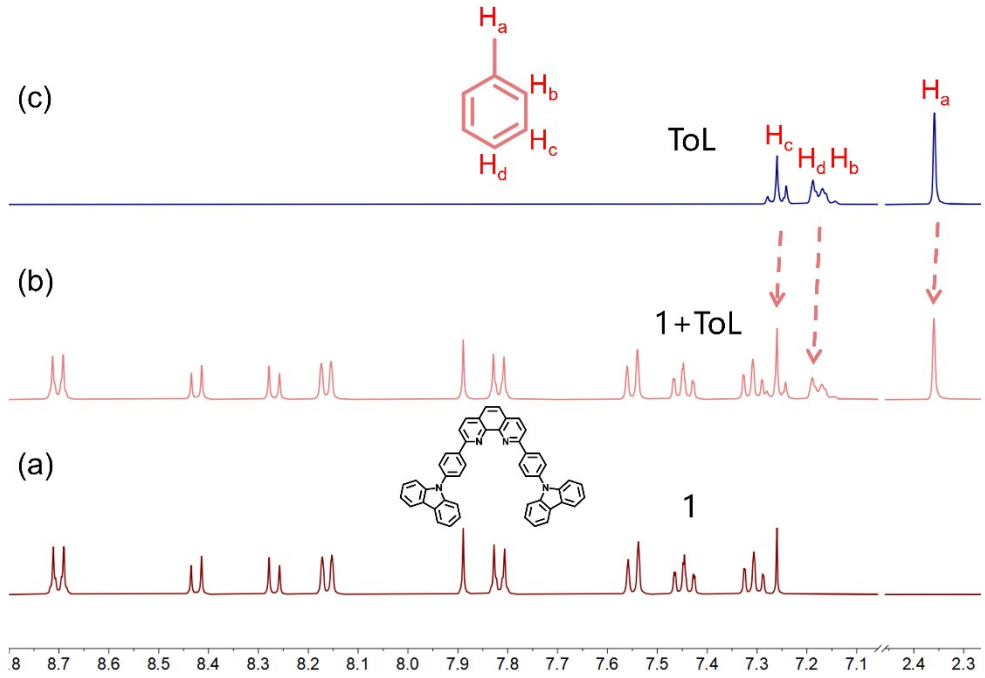

Figure S20. Partial ^{1}H NMR (400 Hz, $CDCl_3$, 298 K) spectra: (a) **1** (9.06 mM); (b) **1** (9.06 mM) and ToL (18.12 mM); (c) ToL (18.12 mM).

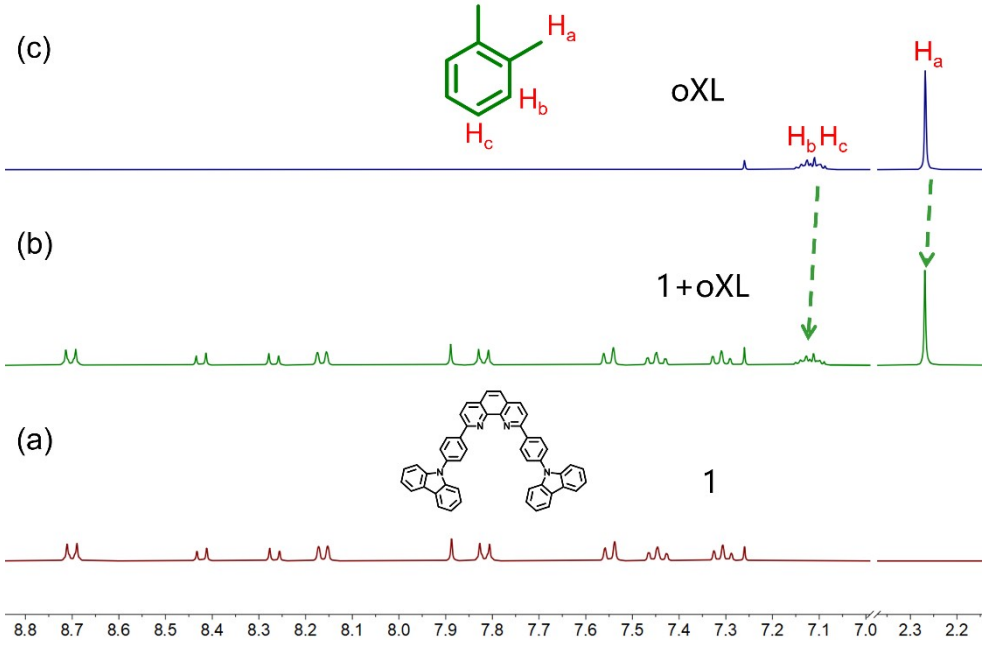

Figure S21. Partial ^{1} H NMR (400 Hz, $CDCl_3$, 298 K) spectra: (a) **1** (9.06 mM); (b) **1** (9.06 mM) and oXL (18.12 mM); (c) oXL (18.12 mM).

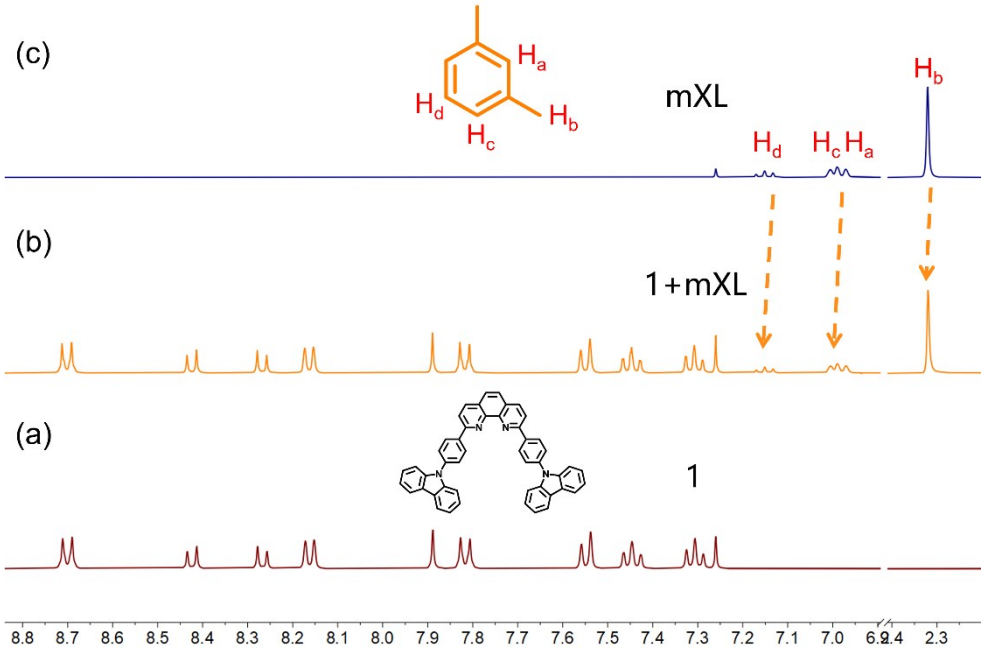

Figure S22. Partial ^{1} H NMR (400 Hz, $CDCl_3$, 298 K) spectra: (a) **1** (9.06 mM); (b) **1** (9.06 mM) and mXL (18.12 mM); (c) mXL (18.12 mM).

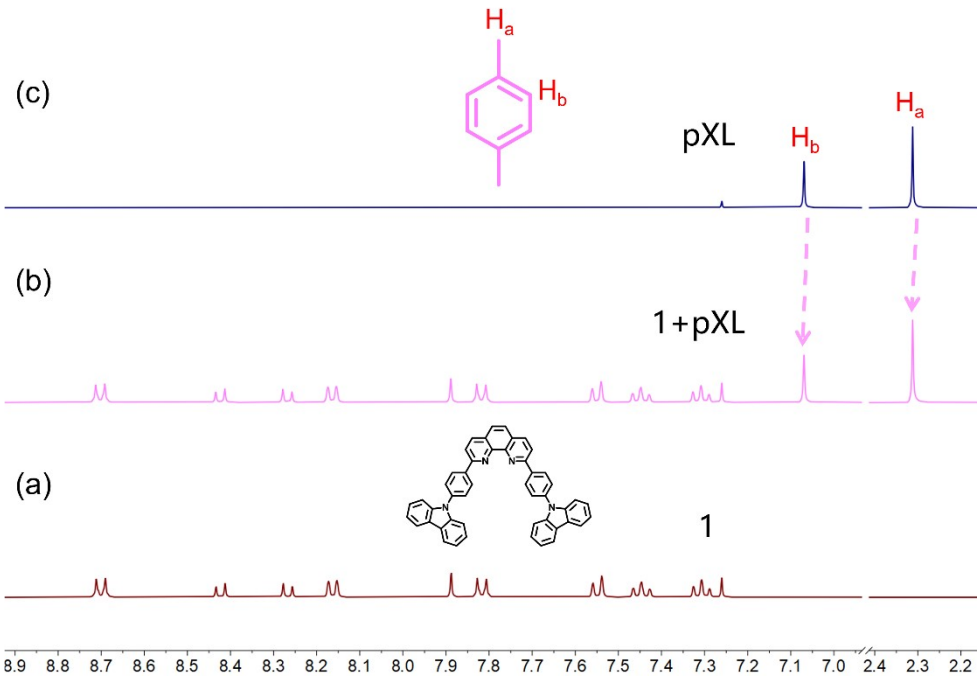

Figure S23. Partial [1] H NMR (400 Hz, $CDCl_3$, 298 K) spectra: (a) **1** (9.06 mM); (b) **1** (9.06 mM) and pXL (18.12 mM); (c) pXL (18.12 mM).

8. Density Functional Theory (DFT) computational data

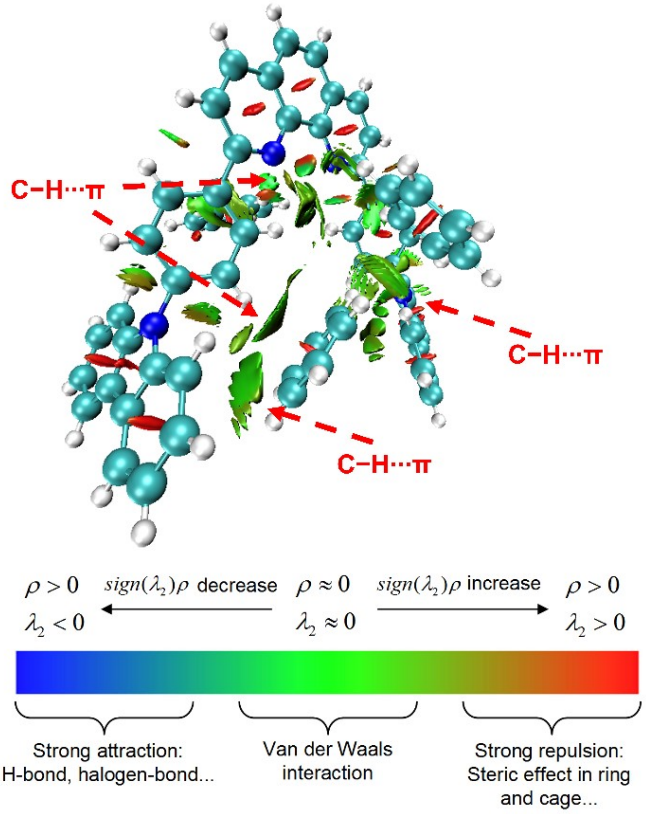

Figure S24. The independent gradient model (IGM) diagram of **Bz@1**.

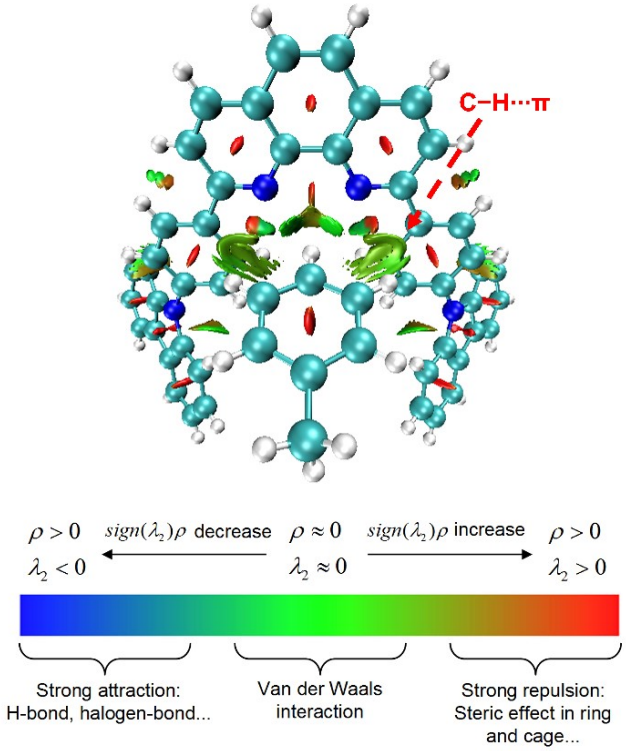

Figure S25. The independent gradient model (IGM) diagram of **Tol@1**.

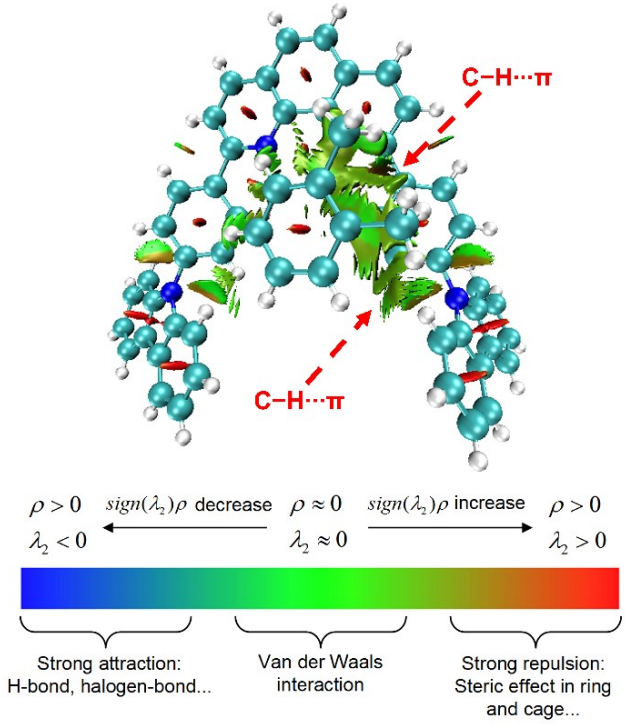

Figure S26. The independent gradient model (IGM) diagram of **oXL@1**.

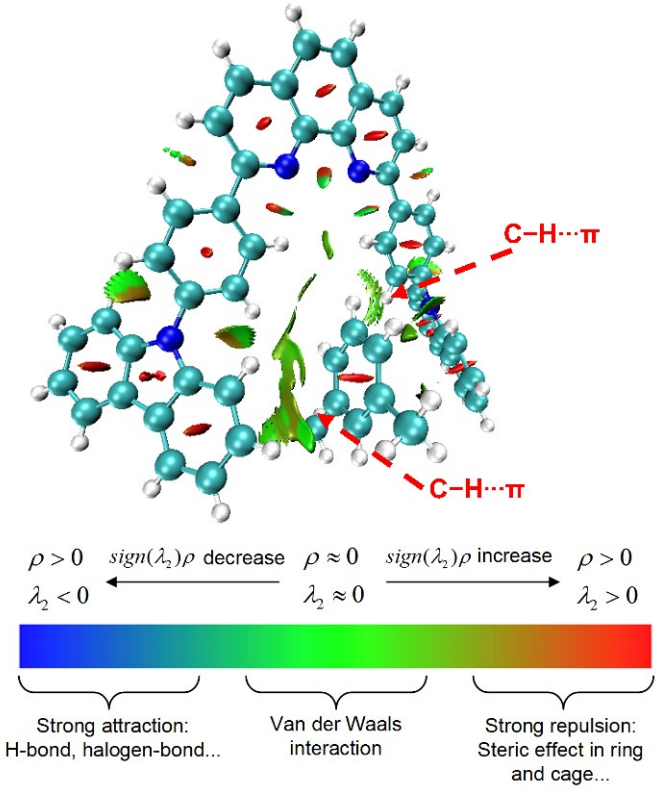

Figure S27. The independent gradient model (IGM) diagram of **mXL@1**.

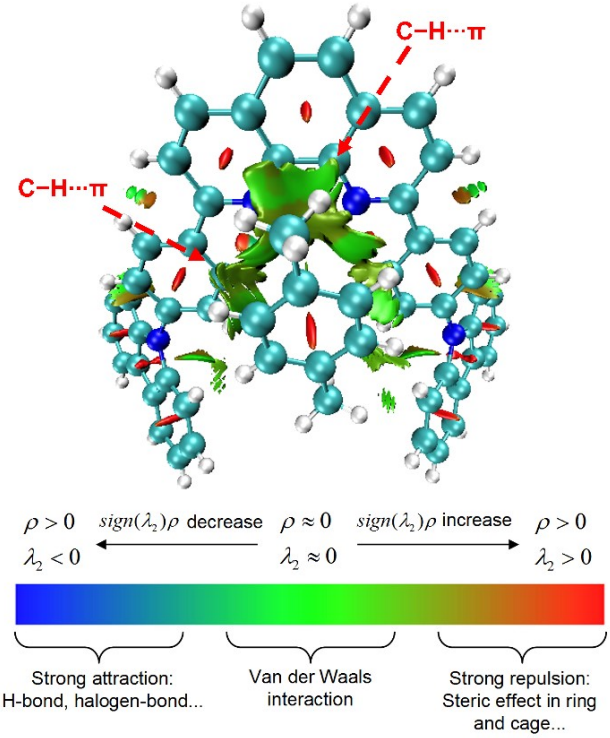

Figure S28. The independent gradient model (IGM) diagram of **pXL@1**.

9. Gas Chromatography-Mass Spectrometry (GC-MS) data

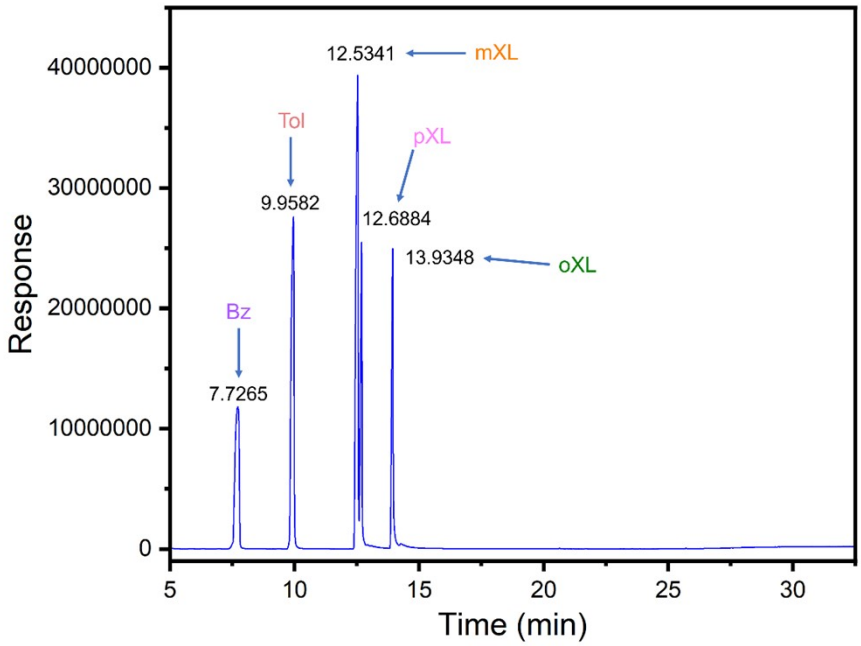

Figure S29. GC diagram of **1-SOFα** fumigated with a mixture of five benzene pollutants for 6 hours.

10. Powder X-ray diffraction (PXRD) data

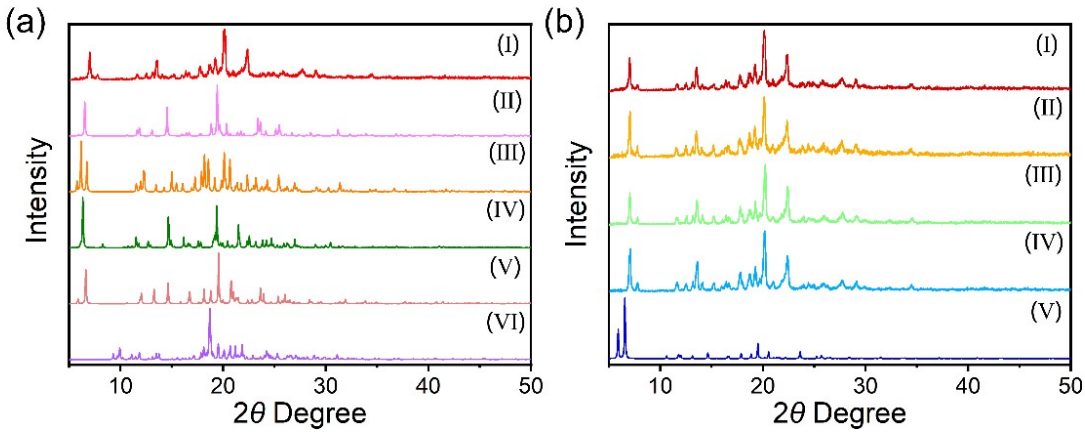

Figure S30. (a) PXRD patterns of **1-SOFα**: (I) after adsorption of five benzene pollutant vapors for 2 h; (II) after adsorption of pXL vapor for 2 h; (III) after adsorption of mXL vapor for 2 h; (IV) after adsorption of oXL vapor for 2 h; (V) after adsorption of ToL vapor for 2 h; (VI) after adsorption of Bz vapor for 2 h**.** (b) Time-dependent PXRD patterns of **1-SOFα** after adsorption of five benzene pollutant vapors for (I) 2 h; (II) 1.5 h; (III) 1 h; (IV) 0.5 h; (V) simulated from single-crystal structure of **1**.

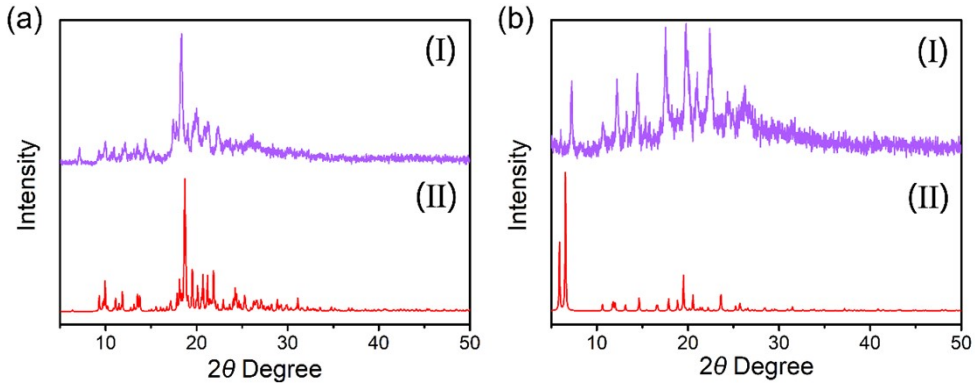

Figure S31. (a) PXRD patterns of **Bz@1-SOFα**: (I) after adsorption of Bz vapor for 2 h; (II) after adsorption of Bz vapor for 2 h simulated from single-crystal structure of **Bz@1**. (b) PXRD patterns of **1-SOFα**: (I) regenerated **1-SOFα** crystals by heating the Bz-adsorbed **1-SOFα** at 100 ºC for 2 hours; (II) simulated from single-crystal structure of **1**.

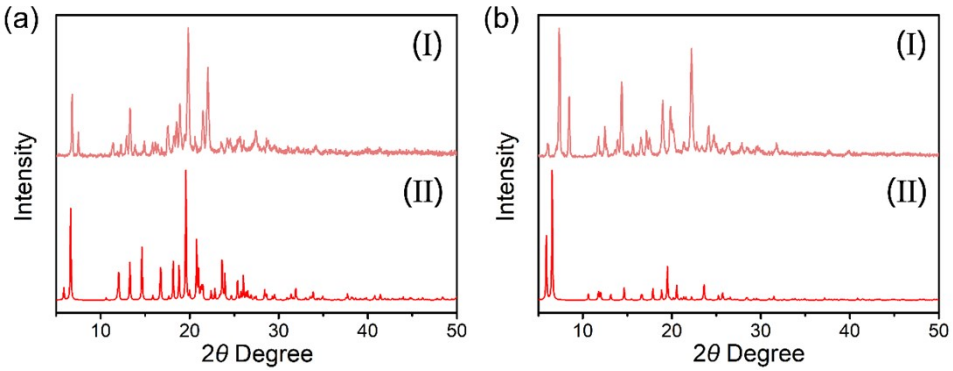

Figure S32. (a) PXRD patterns of **ToL@1-SOFα**: (I) after adsorption of ToL vapor for 2 h; (II) after adsorption of ToL vapor for 2 h simulated from single-crystal structure of **ToL@1**. (b) PXRD patterns of **1-SOFα**: (I) regenerated **1-SOFα** crystals by heating the ToL-adsorbed **1-SOFα** at 100 ºC for 2 hours; (II) simulated from single-crystal structure of **1**.

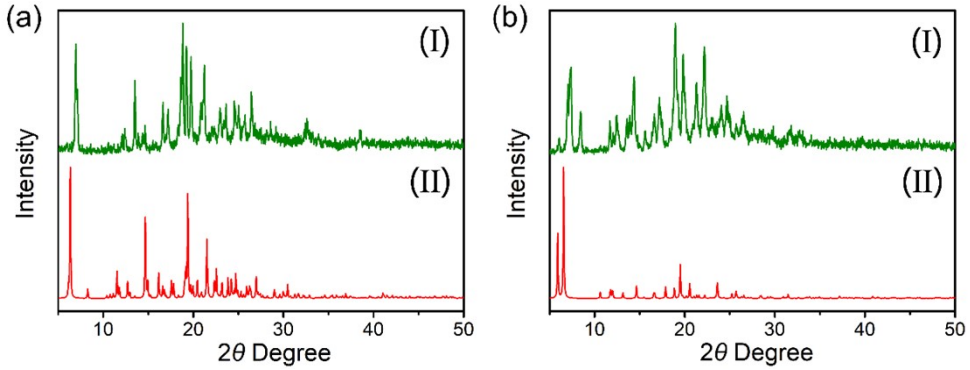

Figure S33. (a) PXRD patterns of **oXL@1-SOFα**: (I) after adsorption of oXL vapor for 2 h; (II) after adsorption of oXL vapor for 2 h simulated from single-crystal structure of **oXL@1**. (b) PXRD patterns of **1-SOFα**: (I) regenerated **1-SOFα** crystals by heating the oXL-adsorbed **1-SOFα** at 100 ºC for 2 hours; (II) simulated from single-crystal structure of **1**.

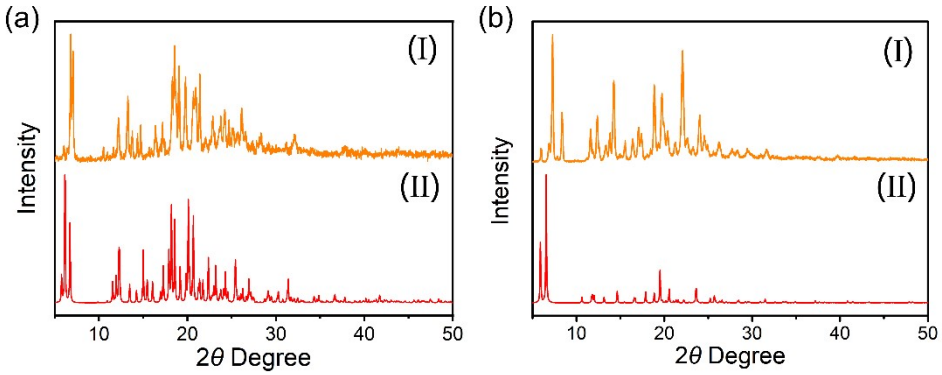

Figure S34. (a) PXRD patterns of **mXL@1-SOFα**: (I) after adsorption of mXL vapor for 2 h; (II) after adsorption of mXL vapor for 2 h simulated from single-crystal structure of **mXL@1**. (b) PXRD patterns of **1-SOFα**: (I) regenerated **1-SOFα** crystals by heating the mXL-adsorbed **1-SOFα** at 100 ºC for 2 hours; (II) simulated from single-crystal structure of **1**.

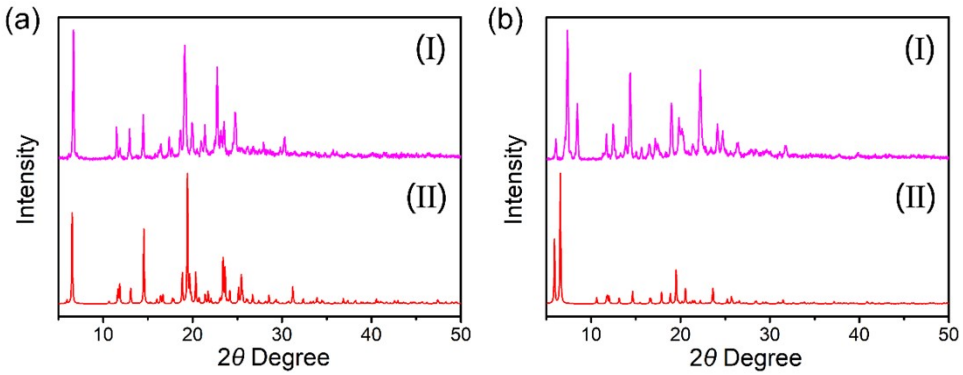

Figure S35. (a) PXRD patterns of **pXL@1-SOFα**: (I) after adsorption of pXL vapor for 2 h; (II) after adsorption of pXL vapor for 2 h simulated from single-crystal structure of **pXL@1**. (b) PXRD patterns of **1-SOFα**: (I) regenerated **1-SOFα** crystals by heating the pXL-adsorbed **1-SOFα** at 100 ºC for 2 hours; (II) simulated from single-crystal structure of **1**.